Journal of Thermal Engineering, Vol. 6, No. 5, pp. 772-785, October, 2020
Yildiz Technical University Press, Istanbul, Turkey

A COMBINED EXPERIMENT-SIMULATION STUDY ON TEMPERATURE REGIME OF ROLLER-COMPACTED CONCRETE APPLYING FOR DAM CONSTRUCTION

Van-Lam Tang[1,2,*], Trong-Chuc Nguyen[3,4], Bulgakov Boris Igorevich[1], Ngoc-Anh Pham[2,5], Trong-Phuoc Huynh[6]

ABSTRACT

Similar to most of the other developing countries, Vietnam has national programs for industrial waste recycling including fuel, ash, and slag. In which, fly ash (FA) has been used commonly as a pozzolanic additive in the roller-compacted concrete (RCC) mixture for the dam construction of hydropower projects. This usage allows reducing the concrete cost, the hydration heat, and the thermal cracking during the construction process of the RCC. In this study, the optimal concrete mixture and the maximum temperature of the RCC dam were determined using the experiment planning method, Matlab, Maple 13, and Midas Civil. In addition, the mathematical model has been used to adequately describe the influence of the intensity concreting (IC) and the initial temperature of the concrete mixture (ITC) on the temperature regime of the RCC dam. The calculation of the temperature regime during the construction of the RCC dam of 45 m high and 1 m thick in Vietnamese climate conditions was performed with considering the IC and the ITC. As the results, the maximum temperature of the RCC dam was determined depending on the IC and the ITC. Calculation found that at IC = 0.6 m/day and ITC = 20°C, the maximum temperature in the central dam zone reached 36.38°C after 1800 hours from the beginning of construction. The results of the present study further support the safe and durable construction of the RCC dam in the future.

Keywords: *Dam, Roller-Compacted Concrete, Compressive Strength, Regression Equation, Response Surface, Contour Plot, Maximum Temperature, Thermal-Stress*

INTRODUCTION

Dam, which is one of the oldest artificial structures, has a responsibility for retaining water in small and large hydropower projects. So far, roller-compacted concrete (RCC) plays an important role in the modern construction of the hydraulic structure. China, a world leader in small and large hydropower projects, is home to the planet's largest hydropower potential at approximately 384 gigawatts, with roughly 20,000 large dams. In China, more than 10 million m3 of the RCC mixture are used annually in the construction of the hydro-technical structure and hydroelectric plants [1,2]. While the first RCC usage for the construction of the hydro-technical dam dates back to 1980 in Japan and about 40 RCC dams have been built [2] after that. Besides, the RCC has been used for building gravity dams in the United States since 1982. In that year, the first RCC dam was completed namely the Willow Creek Dam near Heppner in Oregon [3].

Like other developing countries and emerging economies, there has recently been a great demand for electricity in Vietnam, leading to an unprecedented boom in the construction of hydropower dam, which is also facilitated by the great natural hydropower potential in large power plants. Therefore, the issues of hydropower project construction are very relevant, great economic, and social importance in Vietnam [4–6]. The main characteristics of the five hydroelectric RCC dams in Vietnam recently are given in Table 1. At the same time, the application of RCC technology in the construction of the hydroelectric power project in Vietnam is accompanied by a number of serious problems. One of the major problems is an uncontrolled heat release during the hydration

This paper was recommended for publication in revised form by Regional Editor Erman Aslan
[1]Technology of Binders and Concrete, National Research Moscow State University of Civil Engineering, Moscow, Russian Federation
[2]Faculty of Civil Engineering, Hanoi University of Mining and Geology, No. 18, Pho Vien St., Bac Tu Liem Dist., Ha Noi City, Viet Nam
[3]Hydraulics and Hydraulic Engineering Construction, National Research Moscow State University of Civil Engineering, Moscow, Russian Federation
[4]Institute of Techniques for Special Engineering, Le Quy Don Technical University, No. 236, Hoang Quoc Viet St., Bac Tu Liem Dist., Ha Noi City, Viet Nam
[5]Civil Engineering, Ruhr Universität Bochum, Bochum, Germany
[6]Department of Rural Technology, College of Rural Development, Can Tho University, Campus II, 3/2 St., Ninh Kieu Dist., Can Tho City 900000, Viet Nam
**E-mail address: lamvantang@gmail.com*
Orcid id: 0000-0002-4857-835X, 0000-0001-9723-5161, 0000-0002-4737-8524, 0000-0003-4670-3513, 0000-0003-0657-9159
Manuscript Received 14 October 2018, Accepted 01 January 2019

process of cement, leading to excessive tensile stresses. The reason is that an appearance of extreme thermal gradients in massive hardening concrete leading to thermal cracking in concrete structures [7–10]. In addition, Fu et al. [11,12] reported much information regarding cracks occurring due to thermal stresses. Previous studies reported that the use of fly ash (FA) as a cement substitution resulted in a reduction of hydration heat release, thermal cracking, and production cost of concrete [13–15]. Therefore, FA has been widely used in different massive structures since then [16–18].

Table 1. The main characteristics of the hydropower RCC dams in Vietnam

No.	Dam's name	Compressive strength of RCC		Cement (kg/m^3)	Mineral additives (kg/m^3)		High (m)	Completion year
		MPa	Age (days)		Pozzolan	Fly ash		
1	Pley krong	15	180	80	210	-	75	2009
2	A Vuong	15	180	90	130	-	70	2008
3	Se San 4	15	365	80	120	-	80	2012
4	Ban Ve	17	365	90	130	-	138	2010
5	Son La	16	365	70	-	150	138	2012

In this paper, the preliminary proportion of the RCC mixture was calculated in accordance with the ACI 211.3R-02 standard. The optimal concrete mixture and maximum temperature of the 45 m high RCC dam were determined by the experiment planning method, Matlab computer program, Maple 13 and Midas Civil. Additionally, the mathematical model has adequately described the influence of the intensity concreting (IC) and the initial temperature of the concrete mixture (ITC). Further, the temperature regime of the RCC dam with the optimal proportion was also discussed.

EXPERIMENTAL DETAILS

Materials

Characteristics of the raw materials used in this study were determined in the laboratory according to the guidelines of the related standards with the results as follows:

Type CEM I 42.5 N Portland cement (PC) from But Son factory (Vietnam) was used as a major binder material in RCC mixture. The maximum heat of the cement hydration is 309 J/g at 28 days. The physical and mechanical properties of the PC are presented in Table 2.

Table 2. Physical and mechanical properties of "But Son" Portland cement

Specific gravity	Average diameter of cement grains (μm)	Specific surface area (cm^2/g)	Time of setting (min)		Compressive strength (MPa)			Standard consistency (%)
			Initial	Final	3-day	7-day	28-day	
3.15	29.58	3624	142	235	35.1	40.4	47.3	29.5

The class-F fly ash (FA) sourced from locally TPP Vung Ang (Vietnam) was used as a cement substitution. The volume of the natural porous state is 572 kg/m^3. The chemical compositions and the physical characteristics of the FA are given in Tables 3 and 4, respectively.

Table 3. Chemical compositions of "TPP Vung Ang" FA

Major elements (wt.%)										
SiO_2	Al_2O_3	Fe_2O_3	SO_3	K_2O	Na_2O	MgO	CaO	TiO_2	P_2O_5	LOI [a]
54.62	25.17	7.11	0.85	1.28	0.55	1.57	2.35	1.83	1.63	3.04

[a] LOI = Loss on ignition.

Table 4. Physical properties of “TPP Vung Ang” FA

Sieve size (µm)	10	25	50	75	90
Percentage of passing (%)	1.025	2.812	3.873	27.650	64.640
Mean particle size (µm)	2.588				
Specific surface area (m^2/g)	14.455				
Specific gravity	2.31				

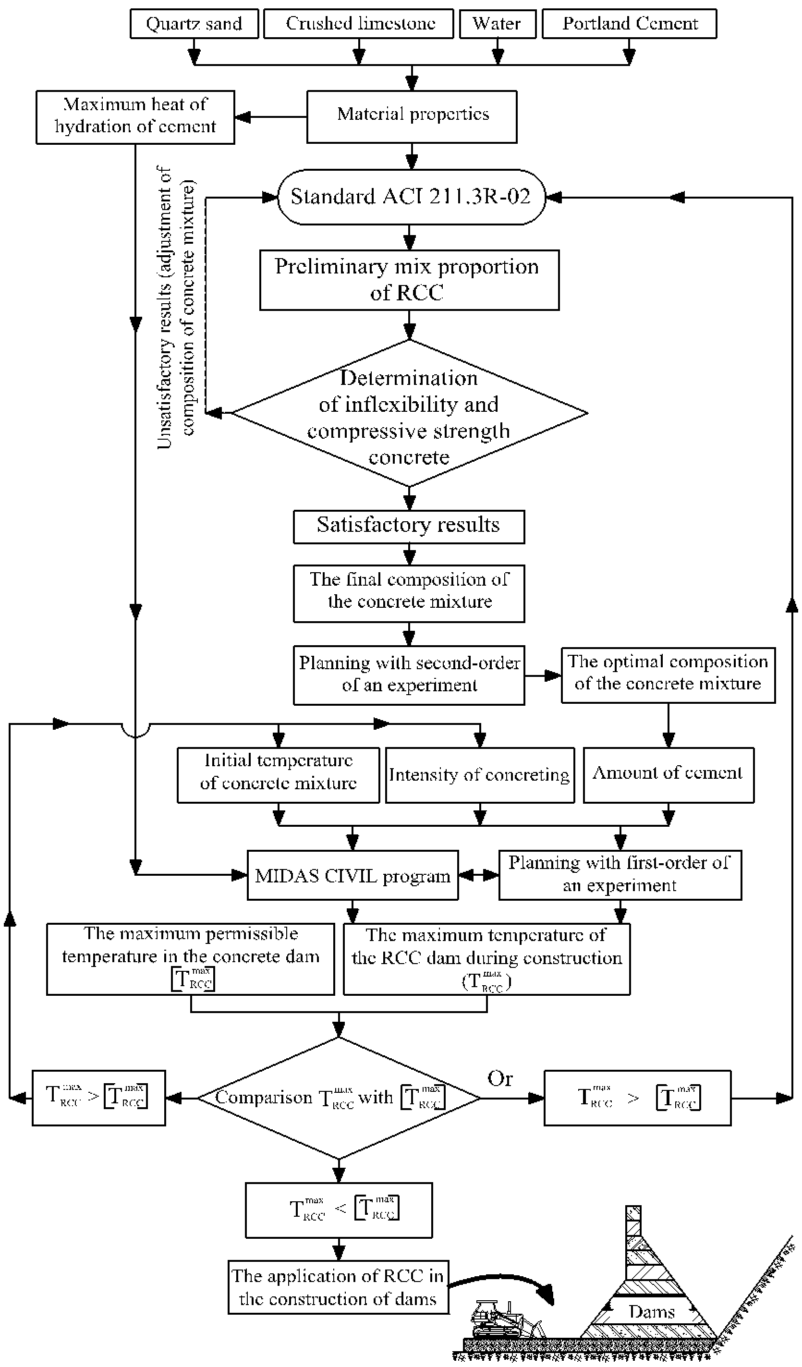

Figure 1. Experimental program

Quartz sand (QS) sourced original from Lo river in Vietnam with the volume of the compacted state is 1650 kg/m^3 was used as fine aggregate in RCC mixtures. The QS had the fineness modulus and density of 3.1 and 2.62 g/cm^3, respectively.

Crushed limestone (CL) sourced from Vietnam with the particle sizes of 5–20 mm and 20–40 mm in a volume ratio of 60:40 and the density of 2.62 g/cm^3 and 2.65 g/cm^3, respectively, was used as coarse aggregate in RCC mixtures.

Local tap water (W) was used for both mixing concrete and curing of the test specimens.

Experimental program

The fully experimental program planning for this study is depicted in Figure 1, in which, the optimal RCC composition was determined by the mathematical experiment planning method with second-order. Mathematical methods are among the most widely used models in operational research and management science. The mathematical-experimental planning method was very useful in performing relationship tests between objects of study and building mathematical programming models or even deciding when such a model is applicable. Furthermore, the Midas Civil computer program based on the finite-element method was used to analyze the thermal behavior of the RCC dam. The desired outcome of this numerical analysis was to determine the spatial distribution of temperature at early-ages and maximum temperatures during the construction process.

Test methods

The preliminary proportion of the RCC mixture was firstly calculated following the procedures as described by ACI 211.3R-02 standard. The workability of the fresh concrete mixture was measured by means of Vebe time in accordance with BS EN 12350-3: 2009. The Ø150 × 300 mm cylindrical concrete specimens were prepared for compressive strength test in according to the guidelines of ASTM C39/C39M-14. The RCC samples were de-molded 24 hours after casting and cured at 20 ± 5°C in a water curing tank until testing time. The compressive strength test was performed at 28 days. The RCC composition was optimized by means of the mathematical experiment planning method with second-order for two factors. The maximum temperature of the RCC dam was calculated using the Midas Civil computer program. Evaluation of crack formation possibility in concrete at an early age was conducted basing on the magnitude of the maximum permissible temperature and maximum temperature arising inside. Effect of the IC and the ITC on the maximum temperature in dam during the construction process was evaluated by the mathematical experiment planning method with first-order for two factors.

RESULTS AND DISCUSSION

Calculation of the preliminary concrete composition

In the case of this study, the RCC properties were selected from the application of RCC technology in the construction of the hydroelectric power project in Vietnam and must possess the following requirements: *(i)* The workability of the RCC that measured by means of Vebe time device ranges from 15 to 20 seconds; *(ii)* The 28-day compressive strength of the RCC is greater than 21 MPa; *(iii)* The RCC has the water-resistant ability in the aquatic environment; *(iv)* FA is used to partially replace PC in the RCC mixture (FA/PC = 1.5 by volume); and *(v)* The relative volume of entrapped air is no more than 1%.

Table 5. Mixture composition and properties of the fresh concrete mixture

Concrete mixture composition (kg/m^3)							Fresh concretes properties			Average compressive strength at 28 days (MPa)
PC	FA	QS	CL			W	Average density (kg/m^3)	[b] W/B	Vebe (s)	
			5-20 (mm)	20-40 (mm)	Total					
101	111	633	928	625	1553	92	2490	1.15	18.5	21.45

[b] W/B is water-to-binder ratio (by volume), where B = PC + FA

Using the ACI 211.3R-02 standard, the preliminary composition of the RCC mixture together with fresh concrete properties and compressive strength of the hardened RCC are presented in Table 5.

Optimization of the RCC composition by mathematical experiment planning method

In this study, the achieved second-order regression equation of the objective function was the compressive strength with the application of the central composite rotatable design (CCRD) method for two factors. The CCRD method allows obtaining more accurate mathematical description by increasing the number of experiments at the center and special value of "star shoulder" $\alpha = \sqrt{2} = 1.414$ [19,20].

Definition of the objective function and input factors for the experimental model description

The compressive strength of the RCC specimen at 28 days, denoted as R_{28}^{RCC} (MPa), is considered as an objective function of this experimental model.

The input variable factors are influenced by the RCC compressive strength, including the weight of each material (PC, QS, CL, W, and FA) required for 1 m^3 concrete. In order to reduce the number of experiments, the weights of QS and CL were fixed to 633 kg/m^3 and 1553 kg/m^3, respectively. Therefore, the input factors and their limitation were chosen as follows:

x_1 = FA/PC (FA-to-PC ratio) ranged from 1.25 to 1.75 by volume.

x_2 = W/B (water-to-binder ratio) ranged from 0.95 to 1.35 by volume.

The input variable factors and their variation intervals are shown in Table 6.

Table 6. Levels and intervals of varying factors of the experimental model

Factors		Levels varying factors					Intervals varying factors δ
Parameters	**Description**	**-1.414**	**-1**	**0**	**+1**	**+1.414**	
FA/PC	x_1	1.25	1.3	1.5	1.7	1.75	0.2 and 0.05
W/B	x_2	0.95	1.0	1.15	1.3	1.35	0.15 and 0.05

Table 7. The matrix of the CCRD for two factors and concrete mixture compositions

Trial No.	Description of code		Compositions of concrete mixtures (kg/m^3)						
	x_1	x_2	PC	FA	B	QS	CL		W
							5-20 (mm)	20-40 (mm)	
1	+1	+1	88	109	197	633	928	625	98
2	-1	+1	103	98	201	633	928	625	98
3	+1	-1	100	125	225	633	928	625	86
4	-1	-1	118	113	231	633	928	625	86
5	+1.414	0	92	118	210	633	928	625	92
6	-1.414	0	112	103	215	633	928	625	92
7	0	+1.414	93	102	195	633	928	625	99
8	0	-1.414	111	122	233	633	928	625	84
9	0	0	101	111	211	633	928	625	92
10	0	0	101	111	211	633	928	625	92
11	0	0	101	111	211	633	928	625	92
12	0	0	101	111	211	633	928	625	92
13	0	0	101	111	211	633	928	625	92

Hence, the number of experiments of the CCRD for the two factors were indicated by formula (1):

$$N = 2^k + 2k + m \qquad (1)$$

where *k* is the number of factors (k = 2) and *m* is the number of trials that repeating at the center (m = 5 as suggested by Terwilliger et al. [21] and Williams [22]). Therefore, $N = 22 + 2\times2 + 5 = 13$.

The RCC compositions that calculated following the ACI 211.3 R-02 standard and central composite rotatable design method of the second-order for two factors are shown in Table 7 and the RCC compressive strength values at 28 days are presented in Table 8.

The second-order regression, equation (2), was obtained from the Matlab computer program. The coefficient values, the response surface image, and the corresponding contour plot are shown in Figure 2.

$$Y_{28} = R_{RCC}^{28} = 22.02 + 2.228x_1 + 0.3427x_2 - 0.43x_1x_2 - 1.144x_1^2 - 0.1757x_2^2 \quad (2)$$

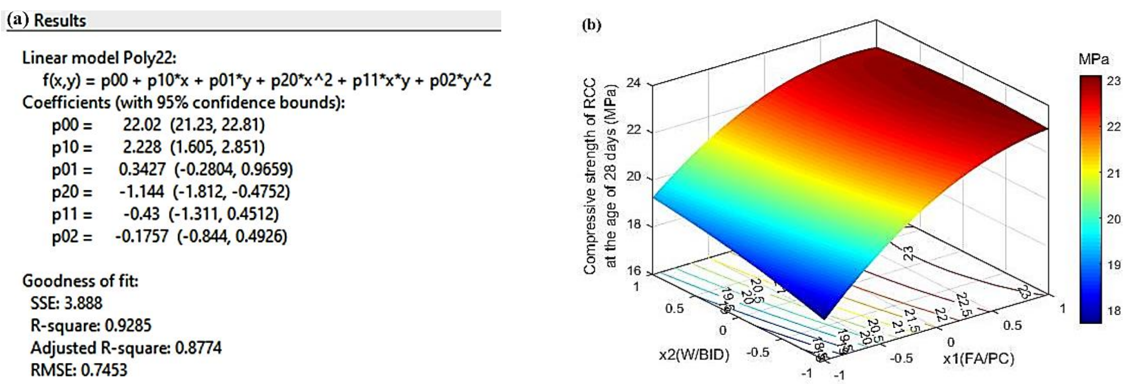

Figure 2. The coefficients (a) and response surface and contour plot of the second-order regression equation (2) for RCC compressive strength at 28 days (b)

Checking the adequacy of this experimental model

The Fisher criterion was used as part of the objective function in the mathematical-experimental method and was used to test regression coefficients for every model. The linear and non-linear parameters of the experimental model were estimated by the root mean square method.

Table 8. Compressive strength of the RCC at 28 days

Trial No.	Description of code						$Y_{28} = R_{28}^{RCC}$ (MPa)		$(Y_{28j}-\hat{Y}_{28j})^2$	$(Y_{028j}-\hat{Y}_{028j})^2$
	x_0	x_1	x_2	x_1x_2	x_1^2	x_2^2	Y_{28j}	$\hat{Y}_{28j}$		
1	+1	+1	+1	1	1	1	23.35	23.24	0.013	-
2	+1	-1	+1	-1	1	1	19.40	18.78	0.384	-
3	+1	+1	-1	-1	1	1	24.02	22.55	2.159	-
4	+1	-1	-1	1	1	1	18.35	18.10	0.065	-
5	+1	+1.414	0	0	2	0	22.05	22.85	0.637	-
6	+1	-1.414	0	0	2	0	16.25	16.55	0.089	-
7	+1	0	+1.414	0	0	2	21.92	22.12	0.039	-
8	+1	0	-1.414	0	0	2	20.25	21.15	0.807	-
9	+1	0	0	0	0	0	22.25	22.02	0.054	0.054
10	+1	0	0	0	0	0	21.98	22.02	0.001	0.001
11	+1	0	0	0	0	0	22.45	22.02	0.187	0.187
12	+1	0	0	0	0	0	21.66	22.02	0.128	0.128
13	+1	0	0	0	0	0	21.75	22.02	0.072	0.072
$\sum(Y_{28j}-\hat{Y}_{28j})^2=4.635$				$S_d^2 = 0.579$			$\sum(Y_{028j}-\hat{Y}_{028j})^2=0.442$			$S_{ll}^2 = 0.110$

According to Wang et al. [23] and Tang et al. [24], the regression equation adequacy was checked by means of the Fisher criterion. The calculated value was indicated by equation (3):

$$F_0 = \frac{S_d^2}{S_{ll}^2} \tag{3}$$

where S_{ll}^2 is variance estimates the experiment reproducibility, determined by equation (4):

$$S_{ll}^2 = \frac{\sum_{j=1}^{m}\left(Y_{oj} - \hat{Y}_o\right)^2}{m-1} \tag{4}$$

where m is the number of repeated experiments at the center (m = 5), Y_{oj} is the obtained value of the ith experiment at the center, $\hat{Y}_0$ is the average value of m experiments at the center, and S_d^2 is estimation of the inadequacy dispersion, determined by equation (5):

$$S_d^2 = \frac{\sum_{j=1}^{N}\left(Y_j - \hat{Y}_j\right)^2}{N-B} \tag{5}$$

where B is the coefficient numbers of the second-order regression equation, which were significant (B = 5), Y_j is the observed value of the ith experiment, and $\hat{Y}_j$ is the obtained value of the experimental function in accordance with the ith experiment.

$F_\alpha\left(f_1, f_2\right)$ is the Fisher criterion value, obtained from Wackerly et al. [25], with a significant level of α = 0.05; f_1 is the number of freedom degrees for residual variance $\left(f_1 = N - B = 13 - 5 = 8\right)$ and f_2 is the number of freedom degrees for estimating the observed variance $\left(f_1 = m - 1 = 5 - 1 = 4\right)$. Therefore, $F_{0.05}$ (8, 4) = 6.041.

For the regression equation (2): $S_d^2 = 0.579$ and $S_{ll}^2 = 0.110$ (Table 8). Then $F_0 = \frac{S_d^2}{S_{ll}^2} = \frac{0.579}{0.110} = 5.244$. As F_0 = 5.244 < $F_{0.05}$ (8, 4) = 6.041, this experimental model described by equation (2) was adequate.

On the other hand, the Maple 13 computer program was used to determine the maximum value of the objective function. The RCC compressive strength at 28 days in the regression equation (2) depended on the input factors of the FA/PC and W/B in the concrete mixture: $Max\ Y_{28}^{Opt} = 23.1155$ at $x_1^{Opt} = 1.02658$ and $x_2^{Opt} = -0.28096$

Then, $Max\ R_{28}^{RCC} = 23.1155\ (MPa)$ at FA/PC = 1.705 and W/B = 1.108 (by volume).

Based on the above calculation, the concrete composition corresponded to the highest RCC compressive strength and optimal dosages of variable components was selected. The material consumption for one cubic meter, which was based on the regression equation (2), is presented in Table 9.

Table 9. The optimum composition of the concrete mixture by using mathematical planning method and the highest compressive strength of the RCC at 28 days

Ratios of raw materials		**Weights of the materials for 1 m³ of concrete (kg)**						**Average density of concrete (kg/m³)**	**Average compressive strength at 28 days (MPa)**	**Average tensile strength at 28 days (MPa)**
FA/PC	**W/B**	**PC**	**FA**	**B**	**QS**	**CL**	**W**			
1.705	1.108	95.15	119	214.15	633	1553	91	2478	24.31	1.95

Mathematical modeling for the effect of the IC and the ITC on the maximum temperature in the RCC dam during the construction process

The Midas Civil computer program was used for determining the maximum temperature of the RCC dam with the optimal concrete mixture as given in Table 9. Simultaneously, using the first-order planning method for two factors, the effect of both the IC and ITC on the maximum temperature in the RCC dam was assessed. According to Aniskin and Chyk [26], the IC values of the RCC dams were selected from 0.2 to 0.6 m/day.

In the RCC dams, the concrete temperature rises from the heat of cement hydration. The quick construction process and low concrete conductivity may be caused by the high thermal gradient in the interior mass and exterior dam surface, as well as thermal-stress. These thermally induced stresses may be significant enough to induce cracks in the RCC dam. The temperature distribution evolution in the dam by time and resulting thermal stress depends on the temperature analysis parameters, such as the environmental conditions, concrete properties, cement amount, lift thickness, temperature, and concrete pouring process [27–30].

RCC dam description

The case study object was an RCC dam in Vietnam with approximately 45 m high and 1 m laid concrete layer thickness. A typical cross-section of the dam is displayed in Figure 3. So far, this hydraulic project, built in the summer, has been playing important roles in flood prevention, sedimentation reduction, irrigation, water supply, and power generation in Northern Vietnam.

According to Aniskin and Chuc [31], the summer temperature in Northern Vietnam change according to equation (6):

$$t_{air} = 25 + 5\sin\left(\frac{2\pi\tau}{24}\right) (^{o}C) \tag{6}$$

where t_{air} is daily average air temperature (ºC) and τ is time (hours).

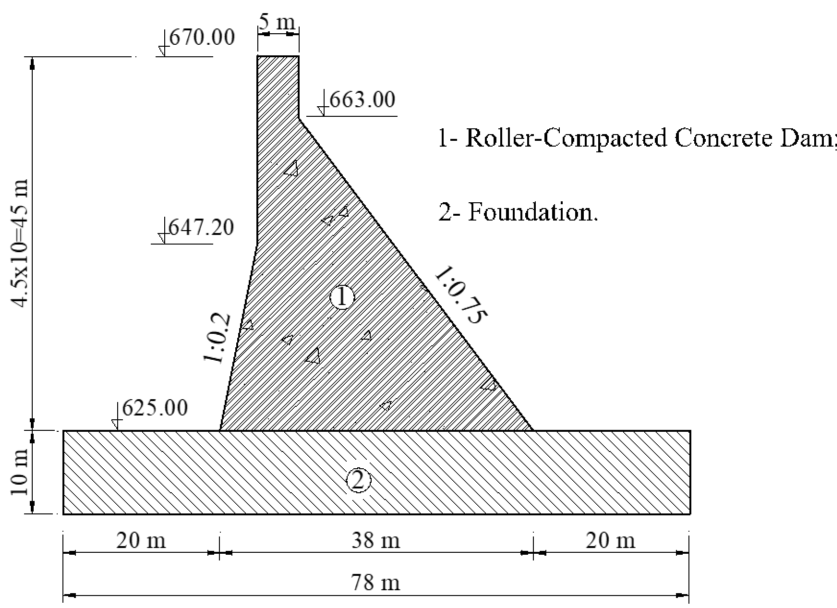

Figure 3. A typical cross-section of RCC dam in Northern Vietnam

The concrete heat release at the instant time τ was determined by equation (7) [27]:

$$q = \frac{1}{24} c.\rho.t_{\max}.e^{\frac{-\alpha\tau}{24}};\ t(\tau) = t_{\max}.\left(1 - e^{-\alpha\tau}\right);\ t_{\max} = \frac{q.PC}{c.\rho} \tag{7}$$

where q is total heat (W/m^3), c is specific heat coefficient (J/kg.^{o}C), PC is cement amount (kg), ρ is concrete density (kg/m^3), $t(\tau)$ is concrete temperature in adiabatic conditions at the age of τ days (^{o}C), t_{max} is temperature rise in the exothermic process under adiabatic conditions (^{o}C), and α is a constant, depending on the concrete mixture casting temperature (α = 0.833, [27]).

Table 10. Properties adopted for temperature analysis

Properties	RCC dam	Foundation
Thermal conductivity coefficient (W/(m.^{o}C)	2.0	3.89
Specific heat coefficient (J/kg.^{o}C)	1.0	0.80
Mass density (kg/m^3)	2490	2700
Coefficient of heat transfer from the exposed surface of concrete-air (W/m^2.^{o}C)	14.47	14.47
Elastic modulus (N/m^2)	2.56.10^{10}	2.0.10^{10}
Thermal expansion coefficient (1/^{o}C)	0.75.10^{-5}	0.75.10^{-5}
Poisson's ratio	0.20	0.20
Maximum cement hydration heat at 28 days (J/g)	309	-
Amount of cement (kg/m^3)	95.15	-
The thickness of the laid concrete layer (m)	1	-

Material properties and environmental conditions

The model attributes were primarily evaluated using the existing data and typical RCC attributes. Table 10 shows the RCC properties and the dam foundation, which were used as inputs to determine the temperature regime in the construction of the concrete dam, including Poisson's ratio, modulus, specific heat, density, and thermal conductivity. The air convection coefficient, which is consistent without the moderate wind speed, was analyzed. Heat generation rate was adopted for the 95.15 kg PC + 119 kg FA in 1 m^3 concrete (as shown in Table 9).

Description of mathematical experiment planning method with first-order

The objective function of this experimental model was the maximum temperature in the RCC dam $\left(Y_i = T_{RCC}^{\max}\right)$ (^{o}C) during the construction process.

The input variables were chosen from the experimental design input parameters as follows:

z_1 - the IC, ranged from 0.2 to 0.6 (m/days).

z_2 - the ITC, ranged from 10 to 20 (^{o}C).

The input variable factors and their variation intervals are shown in Table 11.

Table 11. Levels and intervals of varying variables of the experimental plan method with first-order for two factors

Factors		Levels varying factors			Intervals varying factors δ
Parameter	Description	-1	0	+1	
Intensity concerting (IC)	z_1	0.2	0.4	0.6	0.2
Initial temperature of concrete mixture (ITC)	z_2	10	15	20	5

Table 12. Maximum temperatures occurring in the RCC dam body during construction

Trial No.	Description of code		Parameters		$Y_i = T_i^{max}$ (°C)
	z_1	z_2	IC (m/days)	ITC (°C)	
1	+1	+1	0.6	20	36.38
2	-1	+1	0.2	20	32.35
3	+1	-1	0.6	10	29.30
4	-1	-1	0.2	10	27.37
5	0	0	0.4	15	31.29

The number of necessary experiments (denoted as N) in first-order planning was determined by equation (8):

$$N = 2^k + 1 \tag{8}$$

where k is the number of factors (k = 2) and 1 is the number of this experiment at the center. Hence, $N = 2^2 + 1 = 5$

Figure 4 shows the three-dimensional (3D) finite-element mesh model of the RCC dam. By using the Midas Civil computer program, the maximum temperature that related to the IC and ITC occurring in the RCC dam body during construction time was determined with the values as shown in Table 12 and in Figures 5 – 9.

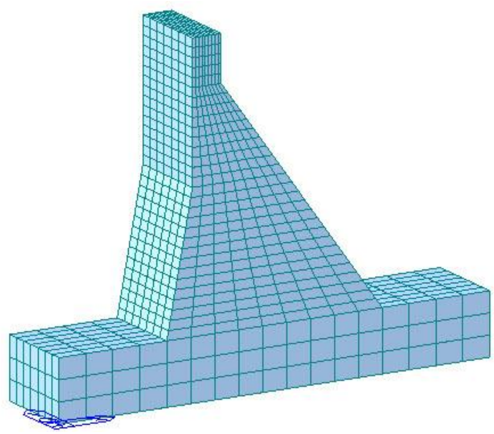

Figure 4. Three-dimensional finite element model mesh

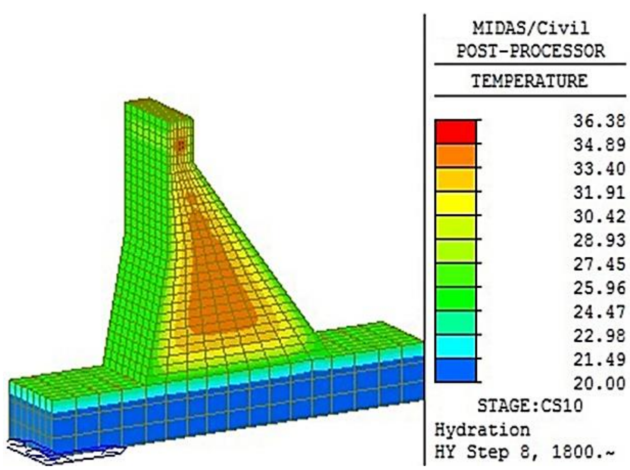

Figure 5. 3D temperature regime process in RCC dam body after 1800 hours from the beginning of construction at IC = 0.6 m/day and ITC = 20°C

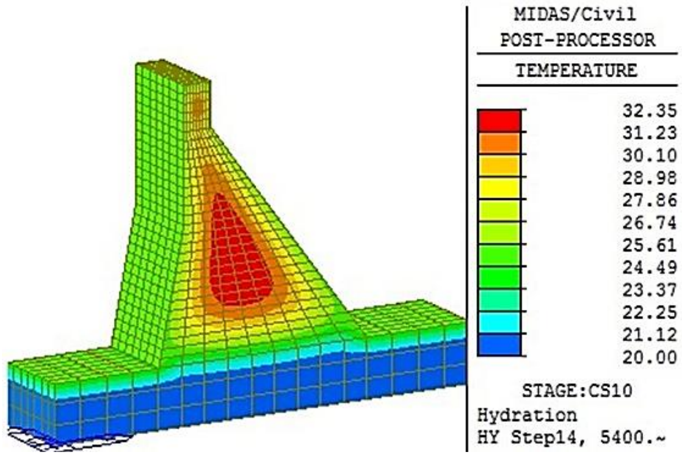

Figure 6. 3D temperature regime process in RCC dam body after 5400 hours from the beginning of construction at IC = 0.2 m/day and ITC = 20ºC

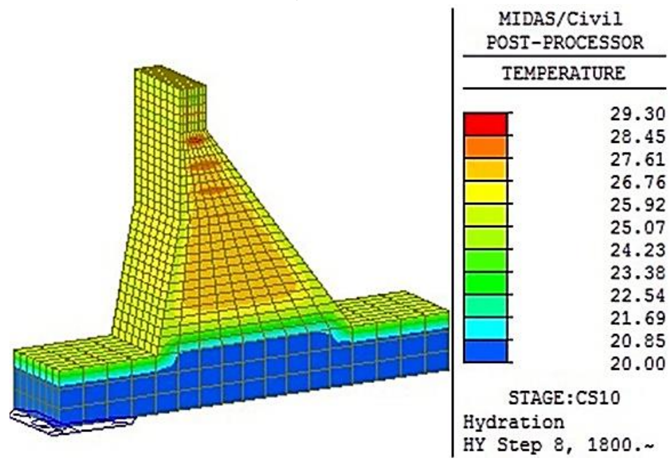

Figure 7. 3D temperature regime process in RCC dam body after 1800 hours from the beginning of construction at IC = 0.6 m/day and ITC = 10ºC

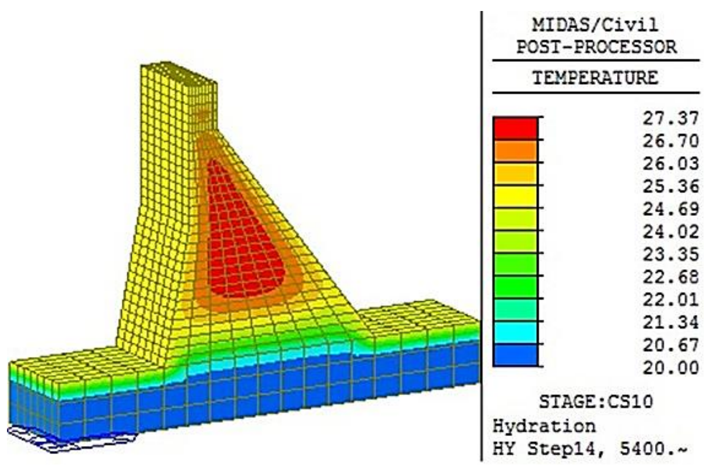

Figure 8. 3D temperature regime process in RCC dam body after 5400 hours from the beginning of construction at IC = 0.2 m/day and ITC = 10ºC

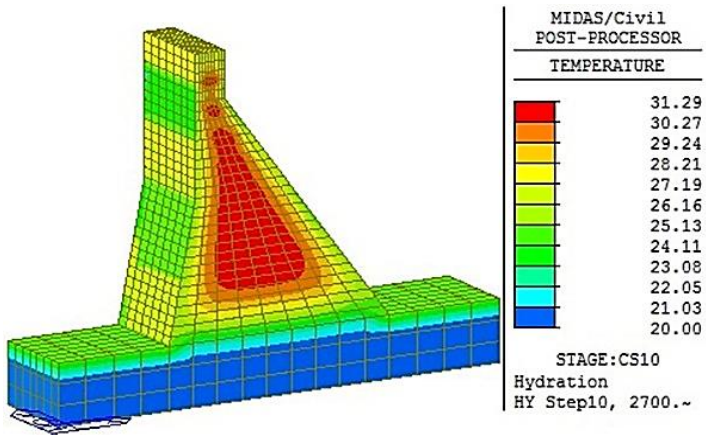

Figure 9. 3D temperature regime process in RCC dam body after 2700 hours from the beginning of construction at IC = 0.4 m/day and ITC = 15°C

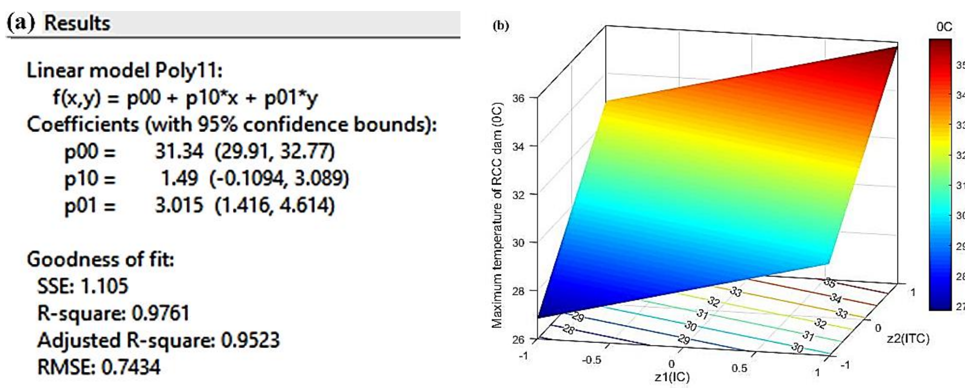

Figure 10. The coefficients (a) and response surface and contour plot of the first-order regression equation (9) for the maximum temperatures during RCC dam construction (b)

Moreover, the Matlab computer program determined the first-order regression equation (9) with the experiment objective function, coefficient values, response surface image, and the corresponding contour plot as presented in Figure 10.

$$T_{\max} = 31.34 + 1.49 z_1 + 3.015 z_2 \tag{9}$$

The first-order regression equation (9) of experimental design showed that the maximum temperature arising in the RCC dam body during construction time increased with the IC and ITC. However, the effect of the ITC was much significant than that of the IC. According to equation (9), the maximum temperature in the RCC dam body obtained during the construction process was 35.85°C at input factors $z_1 = 1$ and $z_2 = 1$.

CONCLUSION

Based on the experiment-simulation results, the following conclusions can be drawn:

The preliminary composition of the concrete mixture with a Vebe time of 18.5 seconds was calculated following the ACI 211.3R-02 standard and the concrete obtained compressive strength value of 21.45 MPa at 28-day.

The composition of the RCC mixture was optimized, based on the second-order regression equation (2) of the RCC, using mathematical planning method for two factors of the Matlab computer program and Maple 13.

The finite-element coding based on the Midas Civil computer program as performed in this study is capable to simulate the thermal response of the RCC dam of 45 m height and 1 m laid concrete layer thickness during well reasonable construction. The maximum temperature of 36.38°C was recorded at the central dam zone after 1800 hours from the beginning of the construction process. In addition, the effects of the IC (z_1) and the ITC (z_2) on the temperature regime of the RCC dam with the optimal concrete composition were simulated by the planning method for two factors and presented by the first-order regression equation (9). According to equation (9), the T_{max}^{RCC} of 35.85°C was found at input factors $z_1 = 1$ and $z_2 = 1$.

By using Midas Civil computer program in combination with the available and full laboratory data, it is possible to simulate the temperature distribution in the RCC dam body during construction time, which can be used in practical applications to avoid the crack appeared in the construction process and ensure the required safety and durability of the constructed hydraulic structures when they get into exploitation and use in the future.

NOMENCLATURE

FA	Fly ash
RCC	Roller-compacted concrete
IC	Intensity concreting
ITC	Initial temperature of the concrete mixture
PC	Portland cement
QS	Quartz sand
CL	Crushed limestone
W	Locally tap water
FA/PC	Fly ash-to-Portland cement ratio
W/B	Water-to-binder ratio
3D	Three-dimensional
CCRD	Central composite rotatable design

REFERENCES

[1] Grumbine RE. Using transboundary environmental security to manage the Mekong River: China and South-East Asian Countries. International Journal of Water Resources Development 2018; 34(5):792–811. https://doi.org/10.1080/07900627.2017.1348938

[2] Zhang S, Yu M, Xiao F, Wang C. Long-term structural responses of orifices in gravity dams considering thermal and creep effects. Journal of Performance of Constructed Facilities 2015;30(3):04015041. https://doi.org/10.1061/(ASCE)CF.1943-5509.0000786

[3] Isao N, Shigeharu J. 30 years' history of roller compacted concrete dams in Japan. Roller compacted concrete dams, Berga et al. edition, Swets & Zeitlinger, Lisse; 2003. http://citeseerx.ist.psu.edu/viewdoc/download?doi=10.1.1.589.3325&rep=rep1&type=pdf

[4] Bui TMH, Schreinemachers P, Berger T. Hydropower development in Vietnam: Involuntary resettlement and factors enabling rehabilitation. Land Use Policy 2013;31:536–544. https://doi.org/10.1016/j.landusepol.2012.08.015

[5] Polimeni JM, Iorgulescu RI, Chandrasekara R. Trans-border public health vulnerability and hydroelectric projects: The case of Yali falls dam. Ecological Economics 2014;95:81–89. https://doi.org/10.1016/j.ecolecon.2013.12.013

[6] Raghavan SV, Tue VM, Yui LS. Impact of climate change on future stream flow in the Dakbla river basin. Journal of Hydroinformatics;16(1):231–244. https://doi.org/10.2166/hydro.2013.165

[7] Liu X, Zhang C, Chang X, Zhou W, Cheng Y, Duan Y. Precise simulation analysis of the thermal field in mass concrete with a pipe water cooling system. Applied Thermal Engineering 2015;78:449–459. https://doi.org/10.1016/j.applthermaleng.2014.12.050

[8] Tressa K, Kavitha PE, Bennet K. Numerical analysis of temperature distribution across the cross section of a concrete dam during early ages. American Journal of Engineering Research 2013;1:26–31. http://www.ajer.org/papers/rase-2013/volume-1/E120132631.pdf

[9] Parveen K, Aeid AA, Bijan S, Khaled G. Thermal and structural response of RCC dams during their service life. Journal of Thermal Stresses 2015;10:1–19. https://doi.org/10.1080/01495739.2015.1015862

[10] Kuzmanovic V, Savic L, Mladenovic N. Computation of thermal-stresses and contraction joint distance of RCC dams. Journal of Thermal Stresses 2013;36(2):112–134. https://doi.org/10.1080/01495739.2013.764795

[11] Fu YF, Wong YL, Tang CA, Poon CS. Thermal induced stress and associated cracking in cement-based composite at elevated temperatures–Part I: Thermal cracking around single inclusion. Cement and Concrete Composites 2004;26:99–111. https://doi.org/10.1016/S0958-9465(03)00086-6

[12] Fu YF, Wong YL, Tang CA, Poon CS. Thermal induced stress and associated cracking in cement-based composite at elevated temperatures–Part II: thermal cracking around multiple inclusions. Cement and Concrete Composites 2004;26:113–126. https://doi.org/10.1016/S0958-9465(03)00087-8
[13] Šavij B, Schlangen E. Use of phase change materials (PCMs) to mitigate early age thermal cracking in concrete: Theoretical considerations. Construction and Building Materials 2016;126:332–344. https://doi.org/10.1016/j.conbuildmat.2016.09.046
[14] Singh PR, Rai DC. Effect of piped water cooling on thermal stress in mass concrete at early ages. Journal of Engineering Mechanics 2018;144(3):0001418. https://doi.org/10.1061/(ASCE)EM.1943-7889.0001418
[15] Modarres A, Hosseini Z. Mechanical properties of roller compacted concrete containing rice husk ash with original and recycled asphalt pavement material. Materials & Design 2014;64:227–236. https://doi.org/10.1016/j.matdes.2014.07.072
[16] Yoshitake I, Komure H, Nassif AY, Fukumoto S. Tensile properties of high volume fly-ash (HVFA) concrete with limestone aggregate. Construction and Building Materials 2013;49:101–109. https://doi.org/10.1016/j.conbuildmat.2013.08.020
[17] Ali MA, Kambiz R. Mechanical properties of high-volume fly ash roller compacted concrete designed by maximum density method. Construction and Building Materials 2013;38:356–364. https://doi.org/10.1016/j.conbuildmat.2012.07.109
[18] Aghabaglou AM, Çakir ÖA, Ramyar K. Freeze–thaw resistance and transport properties of high-volume fly ash roller compacted concrete designed by maximum density method. Cement and Concrete Composites 2013;37:259–266. https://doi.org/10.1016/j.cemconcomp.2013.01.009
[19] Mikulčić H, Klemeš JJ, Vujanović M, Urbaniec K, Duić N. Reducing greenhouse gasses emissions by fostering the deployment of alternative raw materials and energy sources in the cleaner cement manufacturing process. Journal of Cleaner Production 2016;136(Part B):119–132. https://doi.org/10.1016/j.jclepro.2016.04.145
[20] Tang VL, Boris B, Olga A, Oksana L, Pham NA. Effect of rice husk ash and fly ash on the compressive strength of high performance concrete. E3S Web of Conferences 2018;33:02030. https://doi.org/10.1051/e3sconf/20183302030
[21] Terwilliger TC, Bunkóczi G, Hung LW, Zwart PH, Smith JL, Akey DL, Adams PD. Can I solve my structure by SAD phasing? Planning an experiment, scaling data and evaluating the useful anomalous correlation and anomalous signal. Acta Crystallographica Section D: Structural Biology 2016;D72:359–374. https://doi.org/10.1107/S2059798315019403
[22] Williams HP. Model Building in Mathematical Programming. John Wiley & Sons; 2013. ISBN: 978-1-118-44333-0
[23] Wang, B., Xia, X., & Zhang, J. (2014). A multi-objective optimization model for the life-cycle cost analysis and retrofitting planning of buildings. Energy and Buildings, 77, 227–235. https://doi.org/10.1016/j.enbuild.2014.03.025
[24] Tang VL, Boris B, Sofia B, Olga A, Pham NA, Vu DT. Effect of rice husk ash and fly ash on the workability of concrete mixture in the high-rise construction. E3S Web of Conferences 2018;33:02029. https://doi.org/10.1051/e3sconf/20183302029
[25] Wackerly D, Mendenha Ill W, Scheaffer RL. Mathematical Statistics with Applications. Brooks/Cole [Cengage Learning]; 2014. ISBN: 9780495110811
[26] Aniskin N, Chyk NC. Temperature regime of massive concrete dams in the zone of contact with the base. IOP Conference Series: Materials Science and Engineering 2018;365:042083. https://doi.org/10.1088/1757-899X/365/4/042083
[27] Ahmed EYS, Abdelrahman A, Embaby RA. Concrete dams: Thermal-stress and construction stage analysis. Dams and Reservoirs 2017;28(1):1–19. https://doi.org/10.1680/jdare.16.00055
[28] Chen H, Liu Z. Temperature control and thermal-induced stress field analysis of GongGuoQiao RCC dam. Journal of Thermal Analysis and Calorimetry 2018; doi: 10.1007/s10973-018-7450-1. https://doi.org/10.1007/s10973-018-7450-1
[29] Ashtankar VB, Chore HS. Thermo-structural monitoring of RCC dam in India through instrumentation. Structural Monitoring and Maintenance 2015;2(2):95–113. https://doi.org/10.12989/smm.2015.2.2.095
[30] Bobko CP, Zadeh VZ, Seracino R. Improved schmidt method for predicting temperature development in mass concrete. ACI Materials Journal 2015;112(4):579–586. https://doi.org/10.14359/51687454
[31] Aniskin NA, Chuc NT. The thermal stress of roller-compacted concrete dams during construction. MATEC Web of Conferences 2018;196:04059. https://doi.org/10.1051/matecconf/201819604059